Biomaterials 119 (2017) 68–77

Contents lists available at ScienceDirect

Biomaterials

journal homepage: www.elsevier.com/locate/biomaterials

Iron nanomedicines induce Toll-like receptor activation, cytokine production and complement activation

Johan J.F. Verhoef [a, *], A. Marit de Groot [b], Marc van Moorsel [a], Jeffrey Ritsema [a], Nataliia Beztsinna [a], Coen Maas [c], Huub Schellekens [a]

[a] Department of Pharmaceutics, Utrecht Institute for Pharmaceutical Sciences, Utrecht University, Utrecht, The Netherlands
[b] Department of Infectious Diseases and Immunology, Faculty of Veterinary Medicine, Utrecht University, Utrecht, The Netherlands
[c] Department of Clinical Chemistry and Haematology, University Medical Center Utrecht, Utrecht, The Netherlands

ARTICLE INFO

Article history:
Received 13 April 2016
Received in revised form
3 November 2016
Accepted 20 November 2016
Available online 21 November 2016

Keywords:
Iron nanomedicines
Hypersensitivity-like reactions
Innate immune system
Toll-like receptors
Complement activation
Cytokines

ABSTRACT

Approximately a dozen of intravenous iron nanomedicines gained marketing authorization in the last two decades. These products are generally considered as safe, but have been associated with an increased risk for hypersensitivity-like reactions of which the underlying mechanisms are unknown. We hypothesized that iron nanomedicines can trigger the innate immune system. We hereto investigated the physico-chemical properties of ferric gluconate, iron sucrose, ferric carboxymaltose and iron isomaltoside 1000 and comparatively studied their interaction with Toll-like receptors, the complement system and peripheral blood mononuclear cells. Two out of four formulations appeared as aggregates by Scanning Transmission Electron Microscopy analysis and were actively taken up by HEK293T- and peripheral blood mononuclear cells in a cholesterol-dependent manner. These formulations triggered *in vitro* activation of intracellular Toll-like receptors 3, -7 and -9 in a dose- and serum-dependent manner. In parallel experiments, we determined that these compounds activated the complement system. Finally, we found that uptake of aggregation-prone iron nanomedicines by peripheral blood mononuclear cells in whole blood induced production of the proinflammatory cytokine IL-1β, but not IL-6.

1. Introduction

Iron deficiency anemia is a nutritional disorder affecting almost 30% of the world's population [1]. Besides relative low uptake from diet, iron deficiency anemia is seen during pregnancy, hemorrhage and diseases, such as inflammatory bowel disease and chronic kidney failure [2]. Although iron deficiency can be treated with oral iron, patients may require such amounts that are unable to be restored by this route [3]. All commercial intravenous iron formulations consist of a polynuclear Fe(III)-oxyhydroxide/oxide core surrounded by carbohydrates [4]. This carbohydrate shell functions as a stabilizer preventing direct release of bioactive iron and particle aggregation [5]. As such, these products have a diameter between 10 and 30 nm and are considered to be nanomedicines [6]. Examples of carbohydrates used in commercial iron nanomedicines include: sucrose, gluconate, dextran, isomaltoside 1000 and carboxymaltose.

The number of different intravenous iron nanomedicines on the market was limited until the 1990's, but an ever increasing number of products have since entered the clinic [5]. Although iron nanomedicines are considered safe, they are associated with a product dependent risk for (acute) hypersensitivity-like reactions, such as wheezing, bronchospasm, periorbital edema and circulatory collapse; both of which can result in death [7,8]. Although iron dextran is associated with the greatest risk of hypersensitivity-like events, newer developed non-dextran iron nanomedicines are also linked to these reactions, however less frequent [7,9–11]. As such, the European Medicine Agency send out a warning for all commercially available intravenous iron products in 2013 stating that physicians should take precautions when administering these products [12].

Whereas high molecular weight iron dextran formulations have been associated with anti-dextran antibodies, the mechanisms how non-dextran formulations can induce these hypersensitivity-like reactions remain inconclusive [10,13,14]. As such, high molecular weight iron formulations are no longer available [13]. Possible factors triggering these reactions are the release of high

* Corresponding author.
E-mail address: j.j.f.verhoef@uu.nl (J.J.F. Verhoef).

http://dx.doi.org/10.1016/j.biomaterials.2016.11.025
0142-9612/

concentrations of unbound iron into the circulation, recognition of carbohydrates by the immune system and or destabilization of the formulation by dissociation of these carbohydrates [4,9,11,15].

In this study, we investigated the physico-chemical characteristics of four different intravenous iron nanomedicines and their interaction with the innate immune system. We found differences in aggregation behavior among the various formulations investigated which associated with higher cellular uptake and activation of Toll-like receptors, the complement system and specific cytokine release.

2. Materials and methods

2.1. Materials

4-(2-hydroxyethyl)-1-piperazineethanesulfonic acid (HEPES), adenosine triphosphate (ATP), ammonium iron (III) citrate, propidium iodide, chlorpromazine, methyl-beta-cyclodextrin, transferrin, Dulbecco's Phosphate Buffered Saline (PBS) without calcium chloride and magnesium chloride, PBS with calcium chloride and magnesium chloride, fetal bovine serum (FBS), trypsin, ethylenediaminetetraacetic acid (EDTA), RPMI-1640 containing both 20 mM HEPES, L-glutamine and sodium bicarbonate, Dulbecco's Modified Essential Medium containing 4.5 g/L glucose and L-glutamine, and antibiotic–antimycotic solution containing penicillin–streptomycin and antimycotics were all obtained from Sigma-Aldrich (Zwijndrecht, the Netherlands). Ficoll-Paque Plus was obtained from Fisher Scientific (Landsmeer, the Netherlands). Normocin, blasticidin, zeocin, HEk-Blue Selection, PAM3SCK, Poly(I:C) LPS-EK, CL264, ODN2006, and QUANTI-Blue were obtained from Invivogen (Toulouse, France). Ferric gluconate, iron sucrose, ferric carboxymaltose and iron isomaltoside 1000 were kindly provided by Vifor Pharma (Glattbrug, Switzerland) and freshly used before the expiration date. All iron nanomedicines were endotoxin free, determined by the Pyrogene Recombinant Factor C assay (Lonza Benelux bv, Breda, the Netherlands).

2.2. Physico-chemical characterization

Iron nanomedicines were characterized by their mean hydrodynamic particle size and polydispersity index measured by dynamic light scattering (DLS), using a Malvern ALV CGS-3 multiangle goniometer equipped with a He–Ne laser source ($\lambda = 632.8$ nm, 22 mW output power) under an angle of 90° (Malvern Instruments, Malvern, UK). Hydrodynamic size and polydispersity were recorded with an optical fiber-based detector and a digital LV/LSE-5003 correlator with a temperature controller set at 25 °C. Samples were diluted in PBS to 1–2.5 mg iron/mL to realize the highest count rate. Zeta-potential of iron nanomedicines was measured with laser Doppler electrophoresis on a Zetasizer Nano-Z (Malvern Instruments, Malvern, UK) following the diffusion barrier method. A sample of 50 μL was dispersed in 10 mM HEPES buffer pH 7.4 at the bottom of the cell and measured at 150.9 V for 100 runs.

Scanning Transmission Electron Microscopy (STEM) was performed on a Philips 200 kV Tecnai 20F transmission electron microscope (FEI Company, Eindhoven, the Netherlands) equipped with a Field Emission Gun and a Twin objective lens. Images were recorded with a Fischione High Angle Annular Dark Field (HAADF) detector. Energy-dispersive X-ray spectroscopy (EDS) was performed to study chemical composition of the sample. The instrument consisted of a VG Escalab 200 R spectrometer with a MgKα X-ray source ($h\nu = 1253.6$ eV). Iron formulations were diluted to 200 μg iron/mL in dH_2O and 3 μL samples were left to dry on carbon coated copper grids.

2.3. Cell culture

HEK-Blue hTLR cells were cultured in DMEM 4.5 g/L glucose to which 10% FBS, 50 U/mL penicillin, 50 mg/mL streptomycin, 100 μg/mL Normocin and 2 mM L-glutamine was added. HEK-Blue hTLR3 culture medium was supplemented with 30 μg/mL blasticidin and 100 μg/mL zeocin, HEK-Blue hTLR7 and -9 culture medium was supplemented with 10 μg/mL blasticidin and 100 μg/mL zeocin and HEK-Blue hTLR4 culture medium with HEk-Blue Selection.

HEK293T cells were cultured in DMEM with 4,5 g/L glucose supplemented with 10% FBS and an antibiotic–antimycotic solution.

2.4. Toll-like receptor activation reporter assay

Activation of hTLR2, -3, -4, -7 and -9 was investigated using the HEK-Blue hTLR reporter cell-lines (Invivogen, Toulouse, France). HEK-Blue hTLR cells express both a specific hTLR gene and a NF-κB-inducible secreted embryonic alkaline phosphatase (SEAP) reporter gene. HEK-Blue hTLR cells were seeded at assay-dependent amounts (details in Table 1) and incubated overnight with the various iron nanomedicines or positive controls in culture medium.

The next day, SEAP was quantitatively determined by the addition of 20 μL cell supernatant to 180 μL of QUANTI-Blue and incubated for 1 h at 37 °C with 5% CO_2 and subsequently measured at 650 nm using a Biorad Model 550 Microplate Reader (Biorad, Hercules, United States). hTLR activation was expressed by relative alkaline phosphatase levels, defined as sample level divided by PBS control level. Subsequently, synergy between the iron nanomedicines and hTLR agonists was studied by simultaneous incubation of the cells with their specific hTLR agonists and one of the four iron nanomedicines.

hTLR activation without the presence of serum was investigated with HEK-Blue Detection Medium which enables real-time monitoring of SEAP expression without the need for serum. Here, 20 μL sample was added to 180 μL of HEK-Blue Detection Medium and incubated overnight after which absorbance was recorded at 655 nm. SEAP expression was corrected for the absorbance of iron nanomedicines in HEK-Blue Detection Medium.

2.5. Complement activation

Complement activation was investigated by measuring the amount of SC5b-9, a soluble terminal factor released upon activation of either the classical, lectin or alternative pathway. Activation of the alternative pathway was investigated by SC5b-9 analysis in the presence of EGTA/Mg^{2+} and by the detection of the alternative pathway marker Bb. Ferric gluconate, iron sucrose, ferric carboxymaltose and iron isomaltoside 1000 were incubated in 1:4 diluted serum obtained from healthy donors at 500 μg iron/mL. The incubated serum samples were vigorously shaken for 30 min at 37 °C. Negative and positive controls included respectively the incubation with PBS and 200 μg/mL zymosan. SC5b-9 and Bb release were measured by either the MicroVue SC5b-9 Plus or Bb Enzyme

Table 1
Experimental design of the Toll-like receptor activation study using the HEK-Blue hTLR reporter cell-lines.

Cell line	Cells seeded (cells/cm^2)	Positive control
hTLR2	156,250	10 ng/mL PAM3CSK4
hTLR3	156,250	500 ng/mL Poly I:C
hTLR4	78,125	1 ng/mL LPS-EK
hTLR7	250,000	500 ng/mL CL264
hTLR9	250,000	1 μg/mL ODN2006

Immunoassay (Quidel Corp., San-Diego, United States). The samples were diluted 50 fold in the provided reagent diluent supplemented with 25 mM EDTA. The assays were performed according to the manufacturer's protocol.

2.6. Isolation of peripheral blood mononuclear cells

Peripheral blood mononuclear cells (PBMC) were isolated from healthy donors obtained from the mini donor service (MDS) at the University Medical Hospital Utrecht, the Netherlands. Blood was collected in heparinized vacutainers and PBMC were subsequently isolated using a Ficoll-Paque Plus gradient. Briefly, heparinized blood was diluted 1:1 with PBS and subsequently 35 mL of diluted blood was placed on top of 15 mL Ficoll-Paque Plus before centrifugation at 1260 × *g* for 18 min. The PBMC layers were removed, washed in PBS and resuspended in RPMI-1620 supplemented with 10% FBS and an antibiotic-antimycotic solution.

2.7. Cellular uptake of iron NP

Cellular uptake of the iron nanomedicines was investigated in HEK293T cells and PBMC by means of the calcein-AM quenching method, enabling the detection of intracellular ferrous and ferric iron [16,17]. HEK293T cells and PBMC were seeded at respectively 125.000 and 1.562.500 cells/cm^2 in a 96-well plate and incubated at 37 °C under 5% CO_2. The next day, ferric gluconate, iron sucrose, ferric carboxymaltose and iron isomaltoside 1000 were added at concentrations varying between 3.2 and 1000 μg iron/mL. Samples were incubated for 1–7 h at 37 °C with 5% CO_2 and subsequently washed and resuspended in PBS containing Ca^{2+} and Mg^{2+}. Cells were then incubated with 200 μL 12.5 nM calcein-AM in culture medium for 30 min at 37 °C with 5% CO_2. The cells were washed twice with PBS and finally resuspended in PBS before analysis by flow cytometry, using the FACS Canto II (BD Biosciences, San Jose, United States) with a 488 nm solid state laser. Fluorescence intensity was recorded in the green fluorescence channel with 530/30 nm filters. As calcein is quenched by iron, relative uptake of iron nanomedicines was determined as the percentage decrease in calcein fluorescence to the cells treated with PBS. Distinction between quenching in monocytes and lymphocytes was made by means of gating in the FSC/SSC scatter plot.

Endocytic pathway analysis was investigated by pre-incubation of HEK293T cells with 100 μL of either 150-75 μM chlorpromazine, 10 μM methyl-beta-cyclodextrin or 40-10 μM transferrin diluted in culture medium for 30 min. Subsequently, an equal volume of the iron formulations were added and incubated for 1 h. Subsequent calcein-AM staining and analysis was performed as described above.

Cell viability was assessed by staining cells with 2 μg/mL propidium iodide (PI) and subsequent detection by flow cytometry using the FACS Canto II and a 488 nm solid state laser with filters set at 695/40 nm. Viability was expressed as the percentage of gated cells being negative for PI staining.

2.8. Cytokine production in human whole blood

Secretion of IL-1β and IL-6 was studied in blood from 9 healthy donors obtained from the MDS. Blood was collected in heparinized vacutainer tubes and diluted 1:1 in RPMI-1640 supplemented with antibiotics. Diluted whole blood (90 μL) was plated in a 96-well plate and incubated with 10 μL of 3.3–1.000 μg iron/mL ferric gluconate, iron sucrose, ferric carboxymaltose or iron isomaltoside 1000. Controls included PBS and ATP + LPS. Samples were incubated for either 3, 24 or 48 h at 37 °C with 5% CO_2 and centrifuged at 1.500 × *g* for 15 min. Secreted IL-1β and IL-6 were quantified using the human IL-1 beta/IL-1F2 DuoSet and the IL-6 DuoSet (R&D Systems, Abingdon, United Kingdom) according to the manufacturer's protocol.

3. Results

3.1. Physico-chemical characterization of iron nanomedicines

The marketed intravenous iron nanomedicines ferric gluconate, iron sucrose, ferric carboxymaltose and iron isomaltoside 1000 were selected based on their market share, different carbohydrate shielding and stability [4]. As shown in Table 2, neutral zeta-potentials between 0 and -1 mV were measured for all iron nanomedicines in 10 mM HEPES. DLS revealed that z-average, indicating the hydrodynamic diameter, differed among the formulations and ranged between 10 and 25 nm.

STEM analysis revealed that the iron cores of ferric gluconate, iron sucrose and iron isomaltoside 1000 was spherical when dried onto a cupper grid (Fig. 1A, B and D), while the core of ferric carboxymaltose was rod-shaped (Fig. 1C).

Both ferric gluconate and iron sucrose appeared as aggregates, while ferric carboxymaltose and iron isomaltoside 1000 appeared as single particles. STEM revealed core sizes of 9, 6 and 18 nm for ferric gluconate, iron sucrose and ferric carboxymaltose, respectively. Except iron isomaltoside 1,000, all formulations consisted out of monodisperse particles. Here, two populations were identified with an average core size of 3 and 11 nm respectively.

3.2. Toll-like receptor activation by iron NP

Iron nanomedicine therapy is linked to acute hypersensitivity-like reactions which cannot be explained by IgG- or IgE-antibodies [10,14]. We hypothesized that iron nanomedicines can be recognized by means of pattern recognition, an important feature of the innate immune system involved in early inflammatory responses [18]. In our first series of experiments, we investigated the capacity of iron nanomedicines to activate TLRs in HEK-Blue reporter cell lines.

We found that ferric gluconate and iron sucrose, but not ferric carboxymaltose and iron isomaltoside 1,000, activated hTLR3 and to a lesser extend hTLR2, -7 and -9 in a dose-dependent manner (Fig. 2A–E). In these experiments, optical behavior between products was comparable (supporting information S1A), cell viability remained unchanged (supporting information S1B) and activation of hTLR3 and -9 was not observed when cells were incubated with ferric iron only (supporting information S2A and B). No hTLR3 activation was observed when iron nanomedicines were incubated in serum-free medium (supporting information S3), suggesting that a serum co-factor is required for iron nanomedicines to bind hTLRs.

We next studied the interaction between the iron nanomedicines and specific positive control hTLR agonists. We found that ferric gluconate and iron sucrose significantly inhibited the activation of hTLR9 by ODN2006 and to a lesser extent hTLR3 by Poly I:C (Fig. 3A–E).

Table 2
Physico-chemical characterization of four iron nanomedicines.

Sample	Zeta potential (mV)	Z-average (nm)
Ferric gluconate	−0.82 ± 0.05	16.7 ± 0.3
Iron sucrose	−0.86 ± 0.19	12.2 ± 0.5
Feric carboxymaltose	−0.29 ± 0.08	24.3 ± 0.5
Iron isomaltoside 1000	−0.53 ± 0.24	15.4 ± 0.2
10 mM HEPES	−10.13 ± 0.53	–

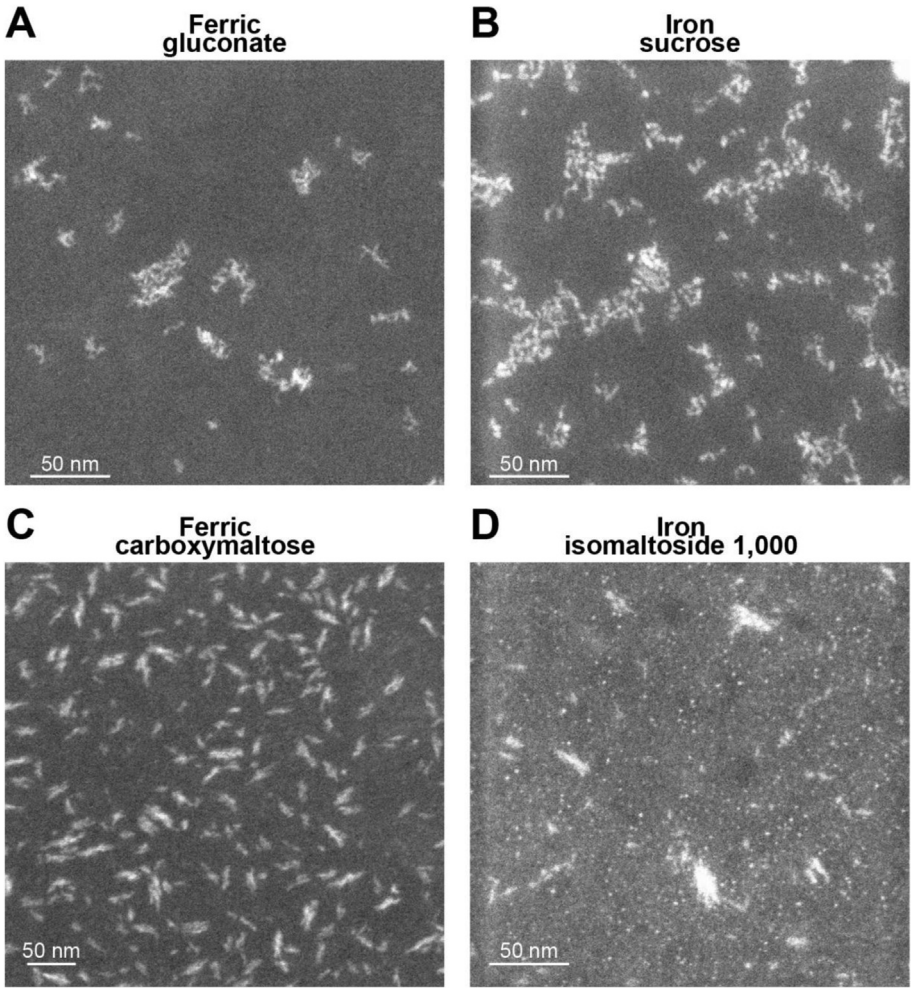

Fig. 1. Imaging of iron oxide cores by Scanning Transmission Electron Microscopy (STEM). Ferric gluconate (A), iron sucrose (B), ferric carboxymaltose (C) and iron isomaltoside 1000 (D) were diluted to 200 μg iron/mL in dH_2O and dried on carbon coated copper grids before analysis.

3.3. Complement activation

Our hTLR data implies that iron nanomedicines are able to adsorb serum proteins necessary for hTLR recognition. Complement factors are part of the innate immune system and play a key role in binding pathogens and damaged cells with the purpose to enhance their recognition and clearance from the circulation by phagocytic cells [19,20]. As such, we investigated if iron nanomedicines can activate the complement system.

Complement activation was assessed in serum obtained from 5 healthy donors. We investigated the appearance of the soluble SC5b-9 and Bb complexes. SC5b-9 is an activation marker of both the classical, lectin and alternative pathway, as it is generated by the assembly of C5 through C9. Bb is an activation fragment of Factor B which only appears upon activation of the alternative pathway. Complement activation through the alternative pathway was also assessed by measurement of SC5b-9 in calcium chelated serum by EGTA/Mg^{2+}. The classical-, and mannose-binding lectin pathway are calcium dependent whereas the alternative pathway can also be activated in the presence of magnesium [21,22].

Sera were incubated with the four different formulations at 500 μg iron/mL. In the donors tested iron sucrose induced significant activation of the complement system determined by SC5b-9 levels compared to ferric carboxymaltose and iron isomaltoside 1000 (Fig. 4A). No SC5b-9 levels were detected in sera incubated with PBS only (data not shown). Ferric gluconate also induced elevated levels of SC5b-9 compared to ferric carboxymaltose and iron isomaltoside 1,000, but were not significantly different ($p < 0.05$). Addition of EGTA/Mg^{2+} diminished SC5b-9 (Fig. 4B), implying that iron nanomedicines induce complement activation in a calcium dependent mechanism which does not rely on the presence of magnesium. This implies that complement activation does not occur through the alternative pathway which was confirmed by the absence of elevated Bb levels above baseline (Fig. 4C).

3.4. Cellular uptake by iron nanomedicines

So far we established that two out of the four iron nanomedicines investigated could activate hTLRs, interfere with specific hTLR positive control agonists and induce complement activation. In human cells, TLR3, -7 and -9 are only expressed intracellularly on endosomal membranes. Hence, physiological activation of hTLRs should only occur when agonists are first taken up by cells.

As such, we investigated intracellular iron in HEK293T cells after 3 h of incubation with the various iron nanomedicines. We determined intracellular iron with a calcein quenching method (more intracellular iron results in higher calcein quenching). Cellular uptake differed substantially between the various iron products (Fig. 5A). In correspondence to our hTLR activation studies in the

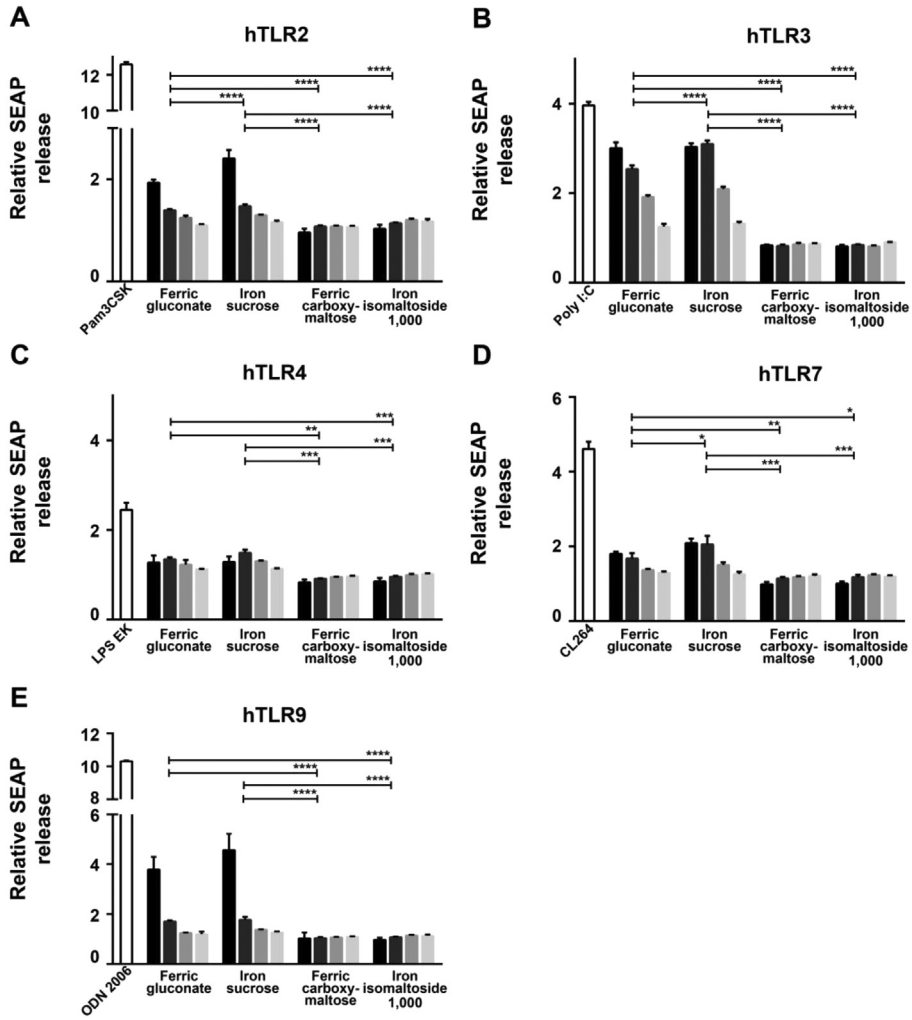

Fig. 2. Activation of Toll-like receptors by iron nanomedicines. hTLR reporter cell-lines were incubated with concentration ranges of ferric gluconate, iron sucrose, ferric carboxymaltose, iron isomaltoside 1000 or positive controls agonists (A– E; black = 1.000 μg/mL, dark grey = 750 μg/mL, middle grey = 500 μg/mL, light grey 250 μg/mL). Data is normalized to PBS-treated cells. Statistical analysis by one-way ANOVA is shown for iron concentrations of 750 μg/mL.

same cell-type, ferric gluconate and iron sucrose were taken up more efficiently than ferric carboxymaltose and iron isomaltoside 1000.

Endocytic pathway analysis on HEK293T cells revealed that uptake by all different formulations was completely inhibited by methyl-beta-cyclodextrin, indicating that uptake of iron nanomedicines occured through the cholesterol mediated pathway. Partial inhibition was observed when the cells were pre-incubated with chloropromazine and transferrin.

Peripheral blood mononuclear cells (PBMC) are important blood-borne mediator cells of innate immune responses and express varies Toll-like receptors. We investigated whether PBMC are able to take up iron nanomedicines. PBMC from healthy donors (n = 5) were incubated for 1, 3 and 7 h. Ferric gluconate and iron sucrose were taken up more effectively than ferric carboxymaltose and iron isomaltoside 1,000, and this difference remained upon 7 h incubation (Fig. 6A–F). Uptake by PBMC occurred preferentially by monocytes.

3.5. PBMC cell viability

PBMC obtained from 3 healthy donors were used to study cell viability after 24 or 48 h incubation. Ferric gluconate and iron sucrose induced a slight decrease in cell viability at 1.0 and 0.1 mg/mL (supporting information S4). No decrease was observed when the cells were incubated with either ferric carboxymaltose or iron isomaltoside 1000.

3.6. Iron nanomedicines trigger cytokine release

Increased cytokine levels in both healthy donors and patients have been reported upon iron administration [15,16,23]. We investigated the release of IL-1β and IL-6 in whole blood supplemented with DMEM containing 4.5 g/L glucose and L-glutamine from healthy donors. IL-1β is a well-known inflammatory marker associated with TLR activation [24]. IL-6 was investigated as increased levels have been reported in patients treated with iron nanomedicines [15].

At baseline, none of the 9 donors had any detectable IL-1β in plasma (data not shown). Most IL-1β production was observed after 48 h incubation when incubated with ferric gluconate and iron sucrose (Fig. 7A–D). No linear dose dependency was observed, instead IL-1β followed an optimum production at 100 μg iron/mL upon incubation with ferric gluconate and at 320 μg iron/mL upon incubation with iron sucrose.

Subsequently, plasma IL-6 levels were analyzed after 24 h

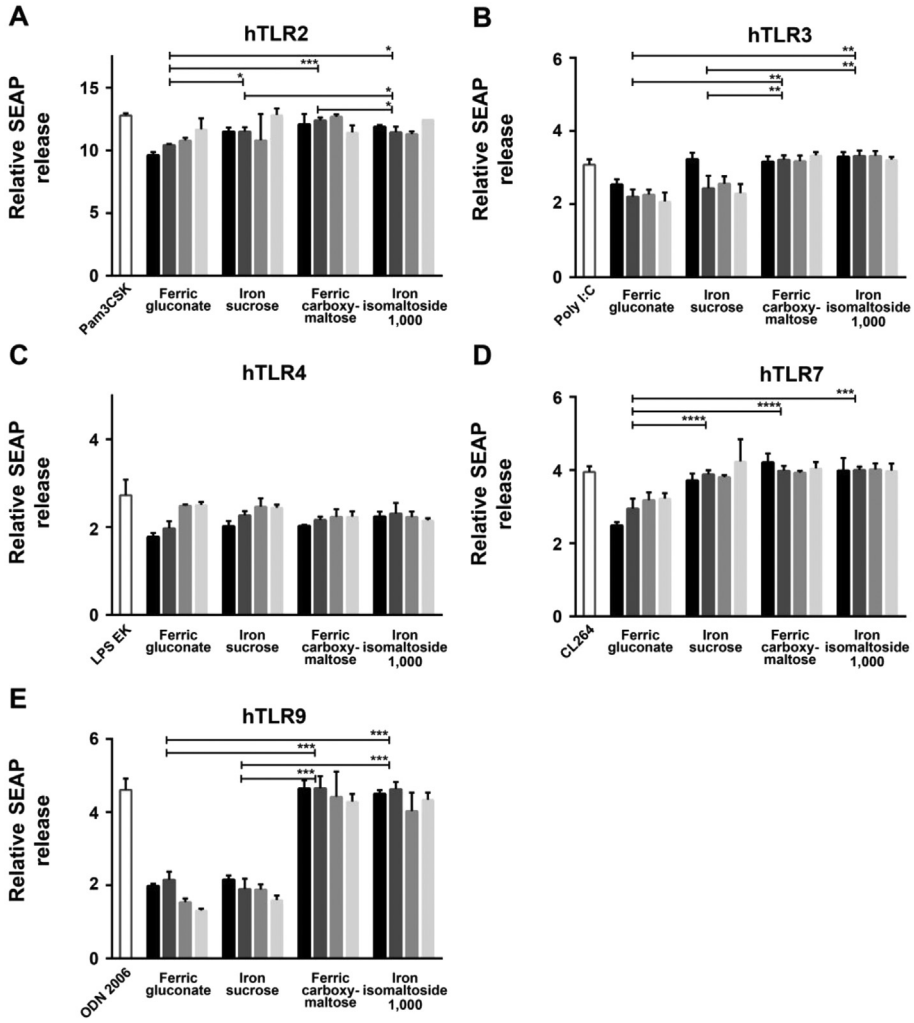

Fig. 3. Interaction between iron nanomedicines and specific positive control agonists during Toll-like receptor activation. hTLR reporter cell-lines were incubated with concentration ranges of ferric gluconate, iron sucrose, ferric carboxymaltose, iron isomaltoside 1000 in the presence of a fixed concentration of a positive control hTLR agonist (A– E; black = 1 mg/mL, dark grey = 750 μg/mL, middle grey = 500 μg/mL, light grey 250 μg/mL). Statistical analysis by one-way ANOVA is shown for iron concentrations of 750 μg/mL.

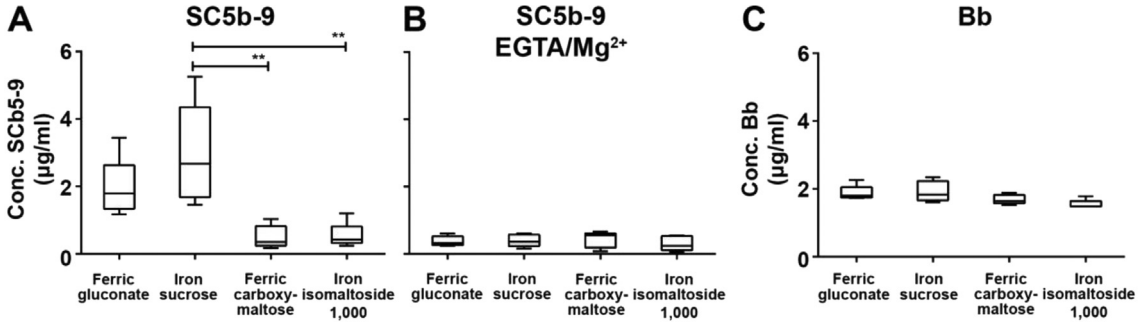

Fig. 4. Complement activation by SC5b-9 and Bb analysis. General complement activation was assessed by measurement of SC5b-9 levels in serum from 5 healthy donors (A). Classical pathway analysis was performed by chelation of Mg^{2+} (B) and measurement of the specific alternative pathway marker Bb (C).

incubation. While IL-1β production mainly occurred when whole blood was incubated with either ferric gluconate or iron sucrose, increased levels of IL-6 were only measured upon incubation with ferric carboxymaltose and iron isomaltoside 1000 (Fig. 8A–D). Here, IL-6 production also did not follow a linear dose dependent relation as an optimum production was found at 100 μg iron/mL upon incubation with iron isomaltoside 1000 and at 320 μg iron/mL upon incubation with ferric carboxymaltose.

4. Discussion

During the last two decades over a dozen of intravenous iron nanomedicines have entered the clinic to treat iron deficiency (anemia), a nutritional disorder affecting almost 30% of the world

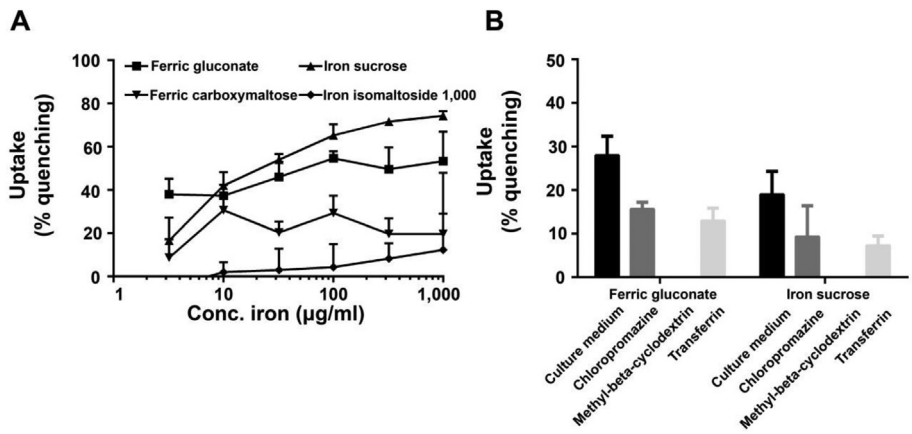

Fig. 5. Iron uptake in HEK293T cells. Uptake was determined by calcein quenching upon 3 h incubation of the various iron nanomedicines (▼ferric carboxymaltose ▲iron sucrose ■ferric gluconate ◆iron isomaltoside 1000) (A). Endocytic pathway analysis was performed by use of the endocytic pathway blockers chlorpromazine, methyl-beta-cyclodextrin and transferrin, respectively known to inhibit clathrin- cholesterol- and transferrin-mediated uptake, on iron uptake (B).

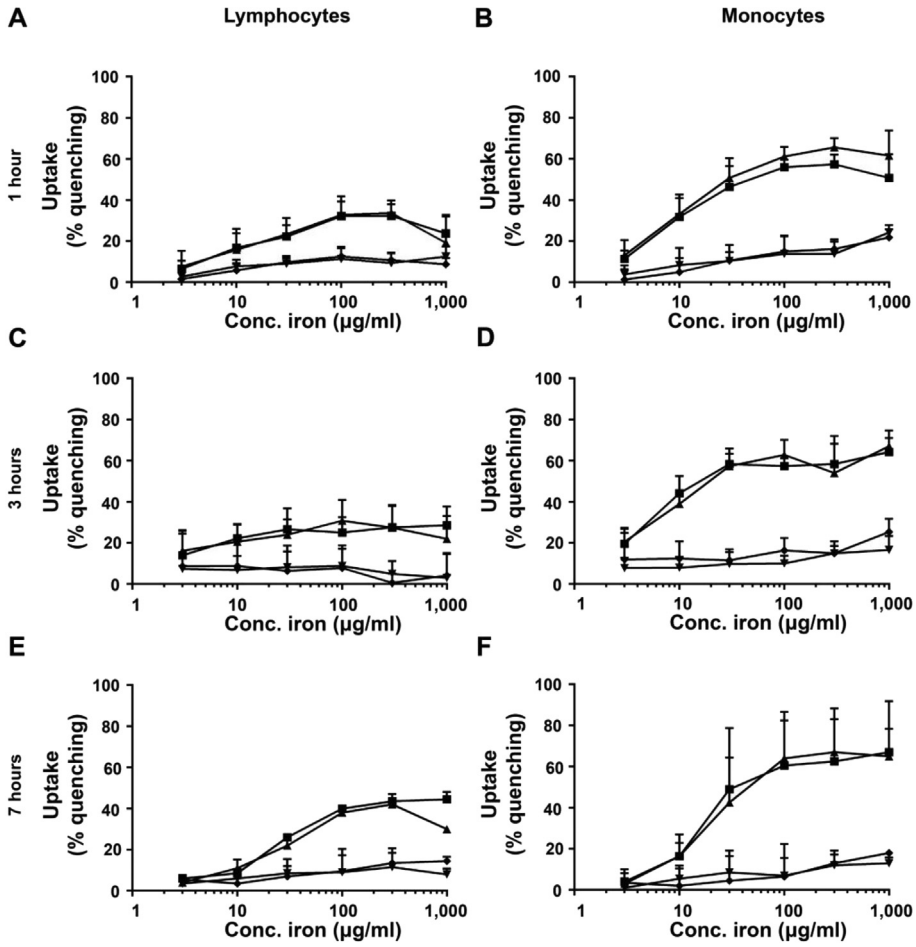

Fig. 6. Iron uptake in PBMC. Uptake was determined by calcein quenching upon 1 (A,B), 3 (C,D) and 7 (E,F) hours incubation of the various iron nanomedicines (▼ferric carboxymaltose ▲iron sucrose ■ferric gluconate ◆iron isomaltoside 1000) in lymphocytes (A,C,E) and in monocytes (B,D,F).

population [1,4]. All these formulations are within the lower nanometer size range and consist of a polynuclear Fe(III)-oxyhydroxide/oxide core surrounded by carbohydrates [4]. Between products, iron cores are not identical and the carbohydrates used to shield the core may differ.

Although administered for many decades, these products are not without safety concerns. For instance, high molecular weight iron dextran products are no longer sold due to severe and sometimes fatal hypersensitivity reactions [5]. In 2013 the European Medicines Agency's Committee for Medicinal Products for Human Use (CHMP) updated their guidelines for all iron nanomedicines with a warning for increased risk of hypersensitivity-like and even

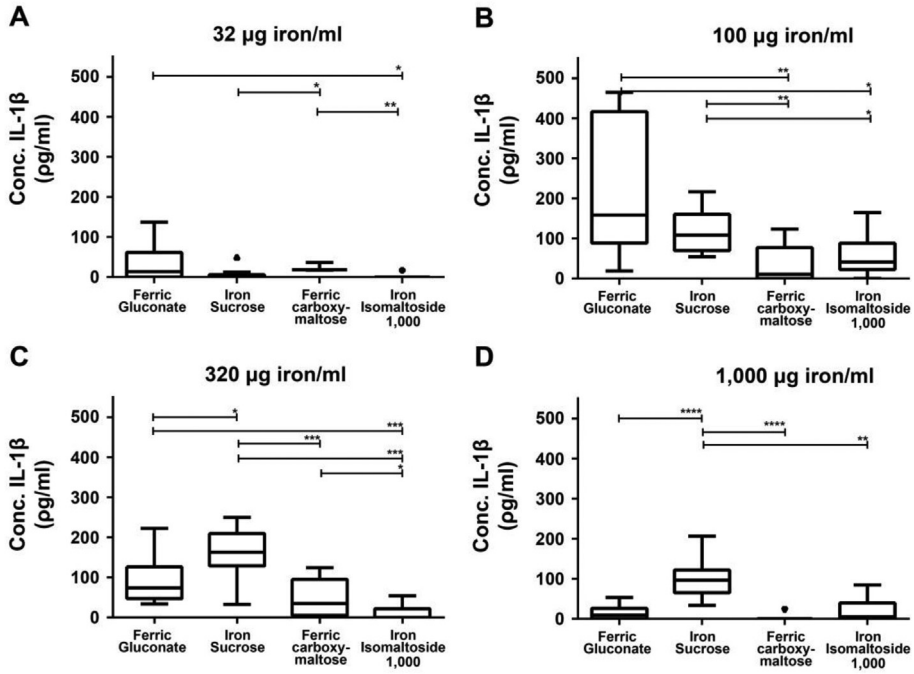

Fig. 7. IL-1β levels in whole blood incubated with various iron nanomedicines. IL-1β release in the extracellular environment was determined upon 48 h incubation of whole blood from healthy donors (n = 9) with the various iron nanomedicines at different concentrations iron (A–D). Statistical analysis was performed by the Mann-Whitney test.

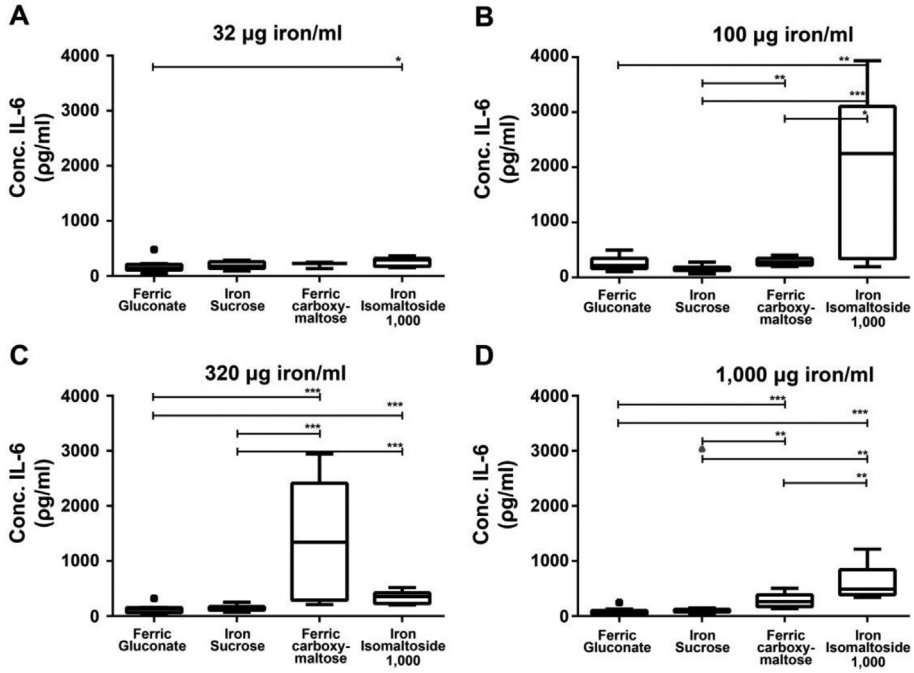

Fig. 8. IL-1β levels in whole blood incubated with various iron nanomedicines. Plasma IL-6 release in the extracellular environment was determined upon 24 h incubation of whole blood from healthy donors (n = 9) with the various iron nanomedicines at different concentrations iron (A–D). Statistical analysis was performed by the Mann-Whitney test.

fatal reactions as well as the necessity to take adequate measures to minimize these reactions [12]. As the rate of new iron nanomedicines entering the market has been increasing over the last decade, it is essential to understand what drives these allergic reactions and how to properly manage them.

The exact mechanisms behind the hypersensitivity-like reactions have not been identified. The induction of radical oxygen species (ROS) as a results of labile iron release has been investigated, but does not appear strictly related and cannot explain these safety issues alone [25]. Pai et al. showed that although iron sucrose and iron dextran show differences in the amount of non-transferrin bound iron in serum, cytokine activation and intracellular ROS generation were essentially similar in PBMC of end-stage renal disease patients [15].

Here, the interaction of four different iron nanomedicines with the innate immune system was investigated as well as their physico-chemical properties. The iron cores of the formulations were in the lower nano-size range and were either spherical or rot-shaped. Size, shape and charge of the iron nanomedicines did not associate with any of the immunological parameters investigated in this paper. However, aggregation behavior associated with substantial hTLR- and complement activation, as well as with cellular uptake and the production of IL-1β, but not IL-6.

Ferric gluconate and iron sucrose appeared as aggregated iron cores when dried onto a grid for STEM analysis. These products induced activation of the endosomal receptors hTLR3 and -7 and were preferentially taken up by both HEK293T cells and PBMC. Surprisingly, ferric gluconate and iron sucrose did not interact directly with hTLRs as no activation was observed when these products were incubated in serum free medium. We hypothesized that these products adsorb serum proteins and opsonins which subsequently can cross-react with endosomal hTLRs.

Ferric gluconate and iron sucrose are known to contain less stable bound carbohydrates which more easily dissociate upon dilution [4]. Ferric carboxymaltose and iron isomaltoside 1000 contain stable bound carbohydrates and are as such shielded against iron core aggregation [4,26]. When products with less stable bound carbohydrates are incubated in serum it is believed that the exposed iron cores adsorb serum proteins and opsonins such as IgG, complement factors and fibrinogen by means of hydrophobic interactions [27–29]. This is supported by the fact that these iron nanomedicines induce complement activation and can scavenge specific positive control hTLR agonists resulting in diminished hTLR activation when incubated together.

Complement activation was assessed by measurement of SC5b-9 levels, a general complement activation marker released upon activation by any of the three complement pathways. We found that ferric gluconate and iron sucrose are able to induce complement activation indicated by elevated levels of SC5b-9. Pathway analysis excluded that ferric gluconate and iron sucrose induce complement activation by the alternative pathway as no SC5b-9 levels were detected when calcium ions were chelated by EGTA. Whereas the classical pathway and mannose-binding lectin pathway require calcium, the alternative pathway requires magnesium. Exclusion of the alternative pathway was confirmed by the fact that no elevated Bb levels were measured, a specific alternative pathway marker. Complement activation therefore occurred either through the mannose-binding lectin- or the classical pathway. Analysis of the classical pathway is preferable performed in sera of treated patients with anti-drug antibodies, which were unavailable for this study. In addition, to our knowledge no reports have been published that identified antibodies against either ferric gluconate or iron sucrose. As such, it is believed that iron nanomedicines can activate the complement system by means of the mannose-binding lectin pathway. These findings are in line with the current concept explaining non-IgE mediated hypersensitivity like reactions observed with several types of nanomedicines, referred to as complement activation-related pseudoallergy (CARPA) [19,30].

Incubation of these products in whole blood resulted in different pro-inflammatory cytokine responses. Whereas cells incubated with ferric gluconate and iron sucrose are more prone to secrete IL-1β; ferric carboxymaltose and iron isomaltoside 1000 mainly secreted IL-6. The inflammatory marker IL-1β is known to be produced by activated PBMC in response to nanoparticulates, such as colloidal aluminum oxide, zinc oxide and urate crystals [24,31,32]. IL-1β is an important cytokine involved in cell proliferation, differentiation and apoptosis.

There is controversy on the exact methods how to characterize the size and charge of iron nanomedicines. As such, different diameters and zeta-potentials have been reported [33,34]. A study by Jahn et al. identified smaller z-averages than presented in this study [34]. In our study, z-averages were measured at higher iron concentration and the dilutions were individually chosen for each product to obtain the highest count rate. Dilution and count rate were found to have a bell curve relation, as dilution decreases both particle concentration and absorption of the laser. With our instrumental setup we found that higher than earlier reported concentrations were needed to obtain a reasonable count rate. Also, zeta-potential was analyzed with a novel method using the diffusion barrier method in 10 mM HEPES which enables a more controlled way of identifying zeta-potentials. This allowed the control of the electrical double layer in contrast to detection in distilled water as reported by others [34,35].

As we have shown in this paper, a head to head comparisons of four different iron nanomedicines showed that these products can interact with the innate immune system. We found that two out of the four formulations appeared as aggregates by Scanning Transmission Electron Microscopy analysis and were actively taken up by HEK293T- and peripheral blood mononuclear cells in a cholesterol-dependent manner. These formulations triggered *in vitro* activation of intracellular TLR3, -7 and -9 in a dose-dependent manner which depended on a serum co-factor. These iron nanomedicines were also able to induce complement activation and were more prone to induce production of the proinflammatory cytokine IL-1beta, but not IL-6 when incubated in whole blood.

The findings in this study reveal another mechanism how iron nanomedicine interact with the immune system. Previous studies have shown that differences in degradation kinetics and the presence of elemental iron is not the sole driver for the hypersensitivity reactions observed in the clinic [15]. In line with this, the findings in this study shed light on the immunological potential of iron nanomedicines by their carbohydrate stability and deserves to be further investigated.

Funding sources

The project was funded by a research grant from Vifor Pharma.

Appendix A. Supplementary data

Supplementary data related to this article can be found at http://dx.doi.org/10.1016/j.biomaterials.2016.11.025.

References

[1] C. Gasche, M.C.E. Lomer, I. Cavill, G. Weiss, Iron, anaemia, and inflammatory bowel diseases, Gut 53 (8) (Aug. 2004) 1190–1197.
[2] J. Umbreit, Iron deficiency: a concise review, Am. J. Hematol. 78 (3) (Mar. 2005) 225–231.
[3] M. Auerbach, et al., Intravenous iron optimizes the response to recombinant human erythropoietin in Cancer patients with chemotherapy-related anemia: a multicenter, open-label, randomized trial, J. Clin. Oncol. 22 (7) (Apr. 2004) 1301–1307.
[4] P. Geisser, S. Burckhardt, The pharmacokinetics and pharmacodynamics of iron preparations, Pharmaceutics 3 (1) (2011) 12–33.
[5] M. Auerbach, H. Ballard, Clinical use of intravenous iron: administration, efficacy, and safety, Hematol. Educ. Program Am. Soc. Hematol. Am. Soc. Hematol. Educ. Program 2010 (2010) 338–347.
[6] B.G. Danielson, Structure, chemistry, and pharmacokinetics of intravenous iron agents, J. Am. Soc. Nephrol. JASN 15 (Suppl 2) (Dec. 2004) S93–S98.
[7] G.R. Bailie, J.-J. Verhoef, Differences in the reporting rates of serious allergic adverse events from intravenous iron by country and population, Clin. Adv. Hematol. Oncol. HO 10 (2) (Feb. 2012) 101–108.
[8] D. Rampton, et al., Hypersensitivity reactions to intravenous iron: guidance for risk minimization and management, Haematologica 99 (11) (Nov. 2014) 1671–1676.
[9] C. Wang, et al., Comparative risk of anaphylactic reactions associated with intravenous iron products, JAMA 314 (19) (Nov. 2015) 2062–2068.
[10] A.J. Bircher, M. Auerbach, Hypersensitivity from intravenous iron products,

Immunol. Allergy Clin. North Am. 34 (3) (Aug. 2014) 707–723 x–xi.
[11] J. Szebeni, et al., Hypersensitivity to intravenous iron: classification, terminology, mechanisms and management, Br. J. Pharmacol. 172 (21) (Nov. 2015) 5025–5036.
[12] European Medicines Agency, New Recommendations to Manage Risk of Allergic Reactions with Intravenous Iron-containing Medicines, 2013 [Online]. Available, http://www.ema.europa.eu/docs/en_GB/document_library/Referrals_document/IV_iron_31/WC500151308.pdf.
[13] R.D. Cançado, M. Muñoz, Intravenous iron therapy: how far have we come? Rev. Bras. Hematol. E Hemoter. 33 (6) (2011) 461–469.
[14] H.S. Novey, M. Pahl, I. Haydik, N.D. Vaziri, Immunologic studies of anaphylaxis to iron dextran in patients on renal dialysis, Ann. Allergy 72 (3) (Mar. 1994) 224–228.
[15] A.B. Pai, T. Conner, C.R. McQuade, J. Olp, P. Hicks, Non-transferrin bound iron, cytokine activation and intracellular reactive oxygen species generation in hemodialysis patients receiving intravenous iron dextran or iron sucrose, Biomet. Int. J. Role Met. Ions Biol. Biochem. Med. 24 (4) (Aug. 2011) 603–613.
[16] L.H. Fell, A.M. Zawada, K.S. Rogacev, S. Seiler, D. Fliser, G.H. Heine, Distinct immunologic effects of different intravenous iron preparations on monocytes, Nephrol. Dial. Transpl. Off. Publ. Eur. Dial. Transpl. Assoc. - Eur. Ren. Assoc. 29 (4) (Apr. 2014) 809–822.
[17] Y. Ma, V. Abbate, R.C. Hider, Iron-sensitive fluorescent probes: monitoring intracellular iron pools, Metallomics 7 (2) (Feb. 2015) 212–222.
[18] O. Takeuchi, S. Akira, Pattern recognition receptors and inflammation, Cell 140 (6) (Mar. 2010) 805–820.
[19] J. Szebeni, Complement activation-related pseudoallergy: a new class of drug-induced acute immune toxicity, Toxicology 216 (2–3) (Dec. 2005) 106–121.
[20] N.K. Banda, et al., Mechanisms of complement activation by dextran-coated superparamagnetic iron oxide (SPIO) nanoworms in mouse versus human serum, Part. Fibre Toxicol. 11 (2014) 64.
[21] D.P. Fine, S.R. Marney, D.G. Colley, J.S. Sergent, R.M. Des Prez, C3 shunt activation in human serum chelated with EGTA, J. Immunol. Balt. Md 1950 109 (4) (Oct. 1972) 807–809.
[22] I. Hamad, A.C. Hunter, J. Szebeni, S.M. Moghimi, Poly(ethylene glycol)s generate complement activation products in human serum through increased alternative pathway turnover and a MASP-2-dependent process, Mol. Immunol. 46 (2) (Dec. 2008) 225–232.
[23] A. Gupta, J. Zhuo, J. Zha, S. Reddy, J. Olp, A. Pai, Effect of different intravenous iron preparations on lymphocyte intracellular reactive oxygen species generation and subpopulation survival, BMC Nephrol. 11 (2010) 16.
[24] H. Li, S.B. Willingham, J.P.-Y. Ting, F. Re, Cutting edge: inflammasome activation by alum and Alum's adjuvant effect are mediated by NLRP3, J. Immunol. 181 (1) (Jul. 2008) 17–21.
[25] A.B. Pai, A.V. Boyd, C.R. McQuade, A. Harford, J.P. Norenberg, P.G. Zager, Comparison of oxidative stress markers after intravenous administration of iron dextran, sodium ferric gluconate, and iron sucrose in patients undergoing hemodialysis, Pharmacother. J. Hum. Pharmacol. Drug Ther. 27 (3) (Mar. 2007) 343–350.
[26] P.A. Kalra, Introducing iron isomaltoside 1000 (Monofer®)—development rationale and clinical experience, NDT Plus 4 (Suppl 1) (Jun. 2011) i10–i13.
[27] D.E. Owens, N.A. Peppas, Opsonization, biodistribution, and pharmacokinetics of polymeric nanoparticles, Int. J. Pharm. 307 (1) (Jan. 2006) 93–102.
[28] H. Carrstensen, R.H. Müller, B.W. Müller, Particle size, surface hydrophobicity and interaction with serum of parenteral fat emulsions and model drug carriers as parameters related to RES uptake, Clin. Nutr. Edinb. Scotl. 11 (5) (Oct. 1992) 289–297.
[29] P. Aggarwal, J.B. Hall, C.B. McLeland, M.A. Dobrovolskaia, S.E. McNeil, Nanoparticle interaction with plasma proteins as it relates to particle biodistribution, biocompatibility and therapeutic efficacy, Adv. Drug Deliv. Rev. 61 (6) (Jun. 2009) 428–437.
[30] J. Szebeni, P. Bedőcs, D. Csukás, L. Rosivall, R. Bünger, R. Urbanics, A porcine model of complement-mediated infusion reactions to drug carrier nanosystems and other medicines, Adv. Drug Deliv. Rev. 64 (15) (Dec. 2012) 1706–1716.
[31] S.C. Eisenbarth, O.R. Colegio, W. O'Connor, F.S. Sutterwala, R.A. Flavell, Crucial role for the Nalp3 inflammasome in the immunostimulatory properties of aluminium adjuvants, Nature 453 (7198) (Jun. 2008) 1122–1126.
[32] Y.-H. Luo, L.W. Chang, P. Lin, Metal-based nanoparticles and the immune system: activation, inflammation, and potential applications, Biomed. Res. Int. 2015 (2015) 143720.
[33] Y. Wu, et al., Core size determination and structural characterization of intravenous iron complexes by cryogenic transmission electron microscopy, Int. J. Pharm. 505 (1–2) (May 2016) 167–174.
[34] M.R. Jahn, et al., A comparative study of the physicochemical properties of iron isomaltoside 1000 (Monofer®), a new intravenous iron preparation and its clinical implications, Eur. J. Pharm. Biopharm. 78 (3) (Aug. 2011) 480–491.
[35] R.B. Shah, Y. Yang, M.A. Khan, A. Raw, L.X. Yu, P.J. Faustino, Pharmaceutical characterization and thermodynamic stability assessment of a colloidal iron drug product: iron sucrose, Int. J. Pharm. 464 (1–2) (Apr. 2014) 46–52.